DOI 10.1007/s11141-015-9600-7
Radiophysics and Quantum Electronics, Vol. 58, No. 4, September, 2015
(Russian Original Vol. 58, No. 4, April, 2015)

COLLISION-INDUCED DIPOLE MOMENT AND MILLIMETER AND SUBMILLIMETER CONTINUUM ABSORPTION IN WATER VAPOR

M. Yu. Tretyakov,[1,2] * **A. A. Sysoev,**[2]
T. A. Odintsova,[1] **and A. A. Kyuberis** [1]

UDC 535.343.4

This work is devoted to estimation of the additional absorption of millimeter and submillimeter wavelengths in water vapor arising from collisional interaction of molecules due to the induced dipole moment. Absorption is modeled on the basis of ab initio *data on the magnitude of the water molecule dipole moment at high densities, and common knowledge of the water vapor absorption spectrum. Using the model developed, we obtained a simple analytical expression for the absorption coefficient as a function of temperature, pressure, and frequency. Comparison of the results with known experimental data leads to the conclusion that in the range of pressures and temperatures typical of water vapor in the Earth's atmosphere this type of absorption is negligible compared with the absorption arising due to association or dimerization of the water vapor molecules.*

1. INTRODUCTION

Study of absorption of the electromagnetic radiation by the Earth's atmosphere is one of the most important applications of modern spectroscopy [1]. In this paper, we consider water vapor as the main absorber of the atmosphere [2]. We analyze the absorption related to the millimeter and submillimeter wavelength ranges, which are used conventionally for remote sensing of the atmosphere [3–7] since the atmospheric transparency in these ranges has a weaker dependence on weather conditions than in the infrared and visible ranges.

Absorption of radiation in a gas can be considered as consisting of the "resonant part," which is composed of the lines corresponding to allowed electric and magnetic dipole transitions, and a "pedestal," which is smoothly varied with the frequency and is called the continuum absorption, or the continuum which is the result of inelastic collisionless interactions of molecules. The continuum is defined as a residue after the "subtraction" of the resonant lines from the total observed absorption.

Considering the collisional interaction of molecules under conditions typical of the Earth's atmosphere, it is possible to confine oneself to the binary interaction of molecules neglecting the higher-order interactions. Therefore, the continuum is generally referred to as resulting from a binary interaction of molecules. There are contributions to the continuum from free molecular pairs and from metastable and bound dimers [8–10]. It should be mentioned that the distant wings of the resonant lines can also contribute to the continuum since all of the currently known analytical forms of the lines used for the absorption calculation were deduced within the framework of the impact approximation, in which the collisions are assumed instantaneous, and

* trt@appl.sci-nnov.ru

[1] Institute of Applied Physics of the Russian Academy of Sciences; [2] N. I. Lobachevsky State University of Nizhny Novgorod, Nizhny Novgorod, Russia. Translated from Izvestiya Vysshikh Uchebnykh Zavedenii, Radiofizika, Vol. 58, No. 4, pp. 287–303, April 2015. Original article submitted June 30, 2014; accepted December 24, 2014.

for the H_2O molecule such a model makes sense only in the vicinity of the center frequency, at about -25 to $+25$ cm^{-1} (± 750 GHz) [11].

Estimation of the contributions from different components of the continuum in different ranges of pressures and temperatures has been the subject of many experimental and theoretical papers (see [9, 10, 12–16, 17] and references therein), from whose results it can be judged which mechanisms dominate in certain conditions. Nevertheless, the discussion of the nature of the continuum continues [18]; therefore, independent estimates of the contributions of different mechanisms remain topical.

In this paper, we analyze the absorption arising due to the interaction of free pairs of water molecules, which results in that an additional dipole moment induced due to the collision exists in each molecule for a short time.[1] The coefficient of this absorption is estimated from the value by which the rotational spectrum of absorption changes during a short-term increase in the dipole moment of the molecules, namely, from

$$\Delta\mu(\rho, T) = \mu(\rho, T) - \mu_0. \tag{1}$$

Here, $\mu_0 = 1.8546(6)$ D is the dipole moment of an isolated water molecule, which was measured experimentally using the Stark effect in [19] and $\mu(\rho, T)$ is the average dipole moment of one molecule as a function of the density ρ and temperature T, with allowance for the interaction of other molecules with the electromagnetic field. The latter is estimated in Sec. 2 on the basis of *ab initio* data presented in [20].

Since normally the interaction of two colliding water molecules is very short-term, the state of the molecule with induced dipole moment has a small lifetime, which is manifested as a large width of the spectral lines. The interaction time is estimated in Sec. 3.

The rotational spectrum $Sp(\nu)$ of the water molecule, which determines the absorption of millimeter and submillimeter waves, is well known and can be modeled from, e. g., the data base [21].

Since the intensity of the rotational spectrum is directly proportional to the molecule's dipole moment squared, the additional absorption coefficient related to the induced dipole moment, α_{ind}, can be estimated from the formula

$$\alpha_{\text{ind}} = \frac{\mu(\rho, T)^2 - \mu_0^2}{\mu_0^2} Sp(\nu). \tag{2}$$

In this case, the width of all lines of the spectrum should be the same and be determined by the average time of collisions. The details of such a modeling are given in Sec. 4.

In Sec. 5, the obtained theoretical results are compared with the experimental data on the continuum absorption in water vapor [22] and the results of [12, 16].

In Sec. 6, we estimate variations in the studied effect on account of the molecule dimerization, since the latter also takes place in the collisional interaction.

In Sec. 7, we substantiate the approach used in this paper.

2. INDUCED DIPOLE MOMENT

The dependence $\mu(\rho, T)$ of the dipole moment of a water molecule on the density and temperature was obtained on the basis of *ab initio* data published in [20]. In the calculations, we used the model in the form of a cube of 64 water molecules under periodic boundary conditions. The cube volume was specified such as the density ρ corresponds to one of the values 1.00, 1.08, 1.25, 1.32, 1.43, and 1.61 g/cm^3. The calculations of molecular dynamics were performed in the Born — Oppenheimer approximation within the

[1] The most complete analysis of the influence of the molecule collisions on the gas absorption spectrum is presented in [23], where the mechanism of the absorption resulting from an inelastic collision of two molecules of the dipole moment (which the authors of [23] called CIA (collision-induced absorption) is mainly regarded as the reason for the occurrence of weak absorption of non-polar gases. However, historically, different groups of spectroscopists use the term CIA to indicate different mechanisms of absorption. Some of them mean the total absorption caused by intermolecular interactions, while others stick to the previous concept, but exclude the contributions of bound dimers, or mean only the absorption related to the collision-induced dipole moment (see [24]). Therefore, to ensure that the terminology is unambiguous, we do not use the term CIA for the absorption in question.

density functional theory [25]. The authors obtained a set of values that characterize the temperature dependence of the average dipole moment of a water molecule in an interval of 300 to 700 K for all the densities considered.

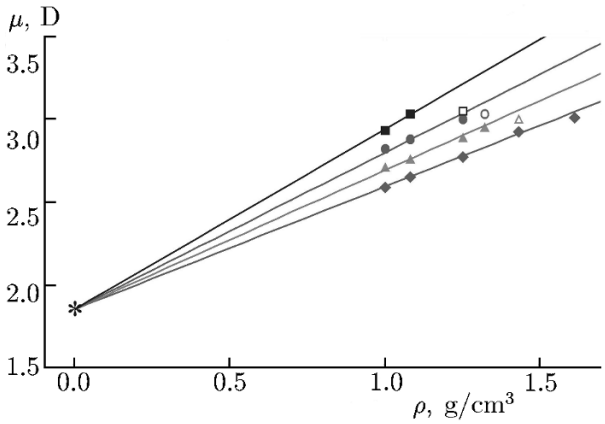

Fig. 1. Dependences of the dipole moment of a water molecule on the density for different temperatures. The symbols from top to bottom show the *ab initio* data [20] for 300, 373, 480, and 700 K. Shaded symbols correspond to the parameters for which the dipole moment variation is mainly determined by binary interactions between molecules. The asterisk denotes the value of the unperturbed dipole moment of the H_2O molecule [19]. Straight lines show the linear approximations of the corresponding *ab initio* data.

The conclusion on the possibility of using the results of the study [20] in this paper can be done on the basis of the analysis of extrapolation of the dependence $\mu(\rho, T = \text{const})$ constructed from the data of [20] to the range of lower densities, in which the binary collision approximation is fulfilled (Fig. 1).

The line $\mu(\rho, T = \text{const})$, which corresponds to the least r.m.s. deviation of all *ab initio* points at a temperature of 700 K (which is by 53 K higher than the critical water temperature), when extrapolated to the zero density gives a value coinciding with the dipole moment of an isolated water molecule within 2%. This indicates that the dipole moment of the molecules changes mainly due to a binary interaction. This conclusion was confirmed by the analysis of the relationship between the coefficients of the virial equation of state of water vapor

$$\frac{pV_\mathrm{m}}{RT} = 1 + \frac{B(T)}{V_\mathrm{m}} + \frac{C(T)}{V_\mathrm{m}^2} + \dots , \tag{3}$$

where p, R, and V_m are the pressure, universal gas constant, and molar volume, respectively, and $B(T)$ and $C(T)$ are the second and the third virial coefficients.

The ratio of the number of triple inelastic collisions of molecules to binary collisions per unit time can be estimated from the ratio of the third term on the right-hand side of virial equation (3) to the second term:

$$\delta(T, \rho) = \frac{C(T)\rho}{B(T)}. \tag{4}$$

Using the parametrization of the virial coefficients of water vapor from [26], it can be shown that at 700 K in the density range 1.00–1.61 g/cm^3 the quantity $\delta(\rho)$ lies within the range 0.013–0.022, i. e., binary collisions really dominate.

For temperatures below the critical one and large densities, this estimation is not possible. Nevertheless, the dependence of the dipole moment on the density at a constant temperature T is linear in a very wide range of densities. From this we can conclude that the dipole moment of a molecule is mainly affected by binary collisions. Note that only the strongest interactions corresponding to the convergence of molecules at a high relative speed with a small impact distance and leading to a significant redistribution of charges in the molecules are of fundamental importance in this paper. In these interactions, short-range repulsive forces come into effect.

To obtain an analytical dependence of the dipole moment of a molecule on the density, the tangent of the inclination angle of the $\mu(\rho, T = \text{const})$ lines best corresponding to the calculated points (shown in Fig. 1 by shaded symbols) was approximated by a simple power-law dependence of the form $(T_0/T)^n$. This yielded the following expression for the dipole moment:

$$\mu(\rho, T)[\mathrm{D}] = \mu_0 + \Delta\mu = 1.8546 + 1.066\rho[\mathrm{g/cm^3}]\,(300/T[\mathrm{K}])^{0.463}. \tag{5}$$

Figure 2 shows that the obtained dependence conforms to the calculated points for two lower densities (1 and 1.08 g/cm^3) considered in [20], for which the effect of intermolecular collisions of a higher order than binary on the dipole moment is the least.

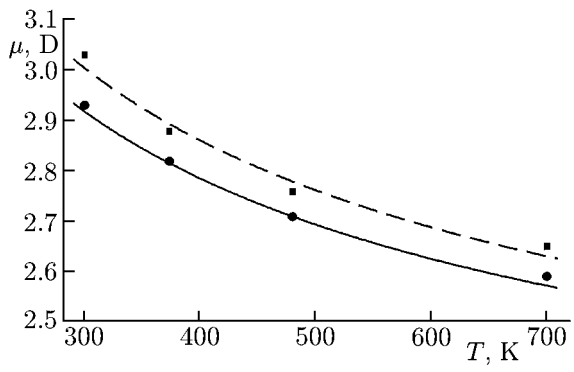

Fig. 2. Dependence of the dipole moment of a water molecule on the temperature T at densities of 1.00 (solid curve) and 1.08 g/cm^3 (dotted curve). The points correspond to the *ab initio* data [20] and the lines, to the calculations based on Eq. (5).

3. TIME OF INTERACTION

The duration of interaction of the colliding molecules is usually estimated as the time of transit of a molecule moving at an average relative thermal velocity by some characteristic distance L, within which this interaction manifests itself. Obviously, the estimate of the transit time is strongly dependent on exactly which interaction is considered and ranges from 10^{-12} to 10^{-13} s (see, e. g., [23] and references therein).

The mean free path λ can be estimated using the formula

$$\lambda = n^{-1/3} = (M/\rho)^{1/3}, \tag{6}$$

where n and ρ are the molecule's concentration and density, respectively, and M is the mass of a water molecule. In the rigid-ball approximation, the radius σ of the excluded-volume sphere can be found as

$$\sigma = \sqrt[3]{\frac{3b_0}{2\pi N_{\rm A}}}, \tag{7}$$

where b_0 is the excluded volume, whose estimate can be found in, e. g., [27], and $N_{\rm A}$ is the Avogadro number. It follows from calculations that for the densities considered in [20], the mean free path coincides, in order of magnitude, with the radius of the excluded-volume sphere. This means that the length of the path of interaction leading to a notable variation in the dipole moment of a molecule can be estimated as a characteristic size of a water molecule, which is of the order of one angström. The interaction time calculated by the formula

$$\tau = \frac{L}{\sqrt{2}}\sqrt{\frac{\pi M}{8kT}} \tag{8}$$

(k is the Boltzmann constant) at temperatures of 300 to 500 K ranges from 0.09 to 0.12 ps.

4. SPECTRUM MODELING

As the basis for modeling of the frequency dependence of the absorption coefficient of this effect, we used the rotational spectrum of an isolated water molecule which is broadened due to a short time of interaction. The spectrum was modeled on the basis of Van Vleck — Weisskopf frequency profiles (9) of the resonance lines

$$\mathrm{line}_{\rm VVW}(I,\nu_0,w,N,\nu) = I\frac{\nu^2}{\pi\nu_0^2}\left[\frac{w}{w^2+(\nu_0-\nu)^2}+\frac{w}{w^2+(\nu_0+\nu)^2}\right] \tag{9}$$

and the full Lorentz form

$$\mathrm{line}_{\rm FL}(I,\nu_0,w,N,\nu) = I\frac{\nu}{\pi\nu_0}\left[\frac{w}{w^2+(\nu_0-\nu)^2}-\frac{w}{w^2+(\nu_0+\nu)^2}\right]. \tag{10}$$

Here, I is the line intensity, ν_0 is the frequency of the line center, N is the concentration of molecules, ν is the frequency, and

$$w = \frac{1}{2\pi\tau}, \tag{11}$$

is the line width determined by the interaction timeτ (i. e., the lifetime of the induced dipole moment).

Function (9) is well suited for modeling of the lines with large width in the millimeter and submillimeter wavelength ranges since initially it was deduced for wide atmospheric lines under conditions where the width of the collisionally broadened line is comparable in magnitude with its center frequency [28]. In this paper, a counterpart for the collisional line broadening (directly related to the time between collisions) is the broadening caused by a short lifetime of the induced dipole moment.

Collisional line form (10) is also suitable in the model considered. In the vicinity of the resonant frequency, functions (9) and (10) virtually coincide, and at frequencies much greater than the frequency of the line center, form (10) yields a more correct asymptotic behavior and, unlike the form (9) from [28], tends to zero, rather than a finite limit.

The expression for the Van Vleck — Weisskopf line form (9) is based on the condition that the thermodynamic equilibrium between the molecule and the radiation is reached immediately after each collision (the collision time is assumed small compared with the oscillation period of the electric field of the wave). The condition of instantaneous collisions permits one to reproduce well the form of the line near its center, but should lead to deviations in the far-wing region when the frequency detuning is comparable with $1/(2\pi\tau)$. Therefore, sometimes a cutoff frequency ν_{cut} is introduced to avoid the physical irrelevance of the far wings of the line, and the line form is written as

$$F^{\text{cut}}_{\text{VVW}}(\nu,\nu_0) = I\frac{\nu^2}{\pi\nu_0^2}[F^{\text{cut}}(\nu,\nu_0) + F^{\text{cut}}(\nu,-\nu_0)], \tag{12}$$

where

$$F^{\text{cut}}(\nu,\nu_0) = \begin{cases} \dfrac{w}{w^2+(\nu_0-\nu)^2} - \dfrac{w}{\nu_{\text{cut}}^2+w^2}, & |\nu-\nu_0| \le \nu_{\text{cut}}; \\ 0, & |\nu-\nu_0| \ge \nu_{\text{cut}}, \end{cases} \tag{13}$$

The last term in the first line of Eq. (13) was entered for the fulfillment of the condition of continuity of the functions for $(\nu-\nu_0) = \nu_{\text{cut}}$. At $\nu_{\text{cut}} \to \infty$, contour (12) converts into the Van Vleck — Weisskopf model given by Eq. (9). The cutoff $\nu_{\text{cut}} = 25$ cm^{-1} (or 750 GHz) is often used in the atmospheric absorption modeling.

In a similar way, the truncated Lorentz form of the line can be written as

$$F^{\text{cut}}_{\text{FL}}(\nu,\nu_0) = I\frac{\nu}{\pi\nu_0}[F^{\text{cut}}(\nu,\nu_0) - F^{\text{cut}}(\nu,-\nu_0)]. \tag{14}$$

Note that such "truncated and tapped" line contours do not satisfy the condition of integrated normalization (i. e., the areas under the contours are not equal to unity). The result is some underestimation of the resonant absorption, which is the greater, the broader the line. This means that the actual dependence of the absorption coefficient on frequency should lie between the model spectra that use complete (Eqs. (9) and (10)) and truncated (Eqs. (12)–(14)) forms of individual lines.

The additional absorption analyzed in this paper is manifested as a result of binary interaction. Since in the ideal-gas approximation the number of molecule pairs is proportional to the pressure squared P^2, it is convenient, for generality of the analysis, to use the normalized absorption coefficient

$$\alpha'_{\text{ind}} = \frac{[\mu(\rho,T)]^2 - \mu_0^2}{\mu_0^2 P^2} Sp(\nu). \tag{15}$$

Expression (15), in view of Eq. (1), can be represented in the form

$$\alpha'_{\text{ind}} = \frac{2\mu_0\,\Delta\mu(\rho,T) + [\Delta\mu(\rho,T)]^2}{\mu_0^2 P^2} Sp(\nu). \tag{16}$$

Under conditions typical of the Earth's ionosphere, the ratio $\Delta\mu(\rho,T)/(2\mu_0)$ is of the order of 10^{-6}, which simplifies Eq. (16):

$$\alpha'_{\text{ind}} = \frac{2\mu_0\,\Delta\mu(\rho,T)}{\mu_0^2 P^2} Sp(\nu). \tag{17}$$

That expression (17) is pressure independent follows from the fact that in the ideal-gas approximation, where the density ρ is proportional to the pressure P, the induced dipole moment $\Delta\mu(\rho,T)$ given by Eq. (1) and the molecule concentration n in the expression for the spectrum are directly proportional to the pressure.

Equation (17), which explicitly includes the total number of gas molecules, does not mean that each collision leads to a notable change in the dipole moment of the colliding molecules. That the absorption coefficient (17) is proportional to the number of molecules follows from the fact that the induced dipole moment calculated in [20] is average per molecule. The rotational spectrum $Sp(\nu)$ of the water molecule in Eq. (17) can, with accuracy sufficient for this problem, be represented as the sum of all known lines of the basic isotopologue $H_2{}^{16}O$ in the frequency range 0–750 cm^{-1} (it is exactly the frequency range that includes all the lines that give a significant contribution to the rotational spectrum) in accordance with the spectroscopic data base [21].

The results of calculation of studied absorption coefficient (17) using full (Eqs. (9) and (10)) and truncated (Eqs. (12)–(14)) line forms are presented in Fig. 3.

As was expected, the use of truncated line forms gives a much smaller absorption coefficient compared with the full form, but does not change qualitatively the common shape of the frequency dependence. The overestimated absorption coefficient obtained in the range of high frequencies using the full Van Vleck — Weisskopf line form (9) compared with the case of using the full Lorentz form is a well-known feature of the line form (9) stipulated by the assumptions made when it was obtained [28]. An equally well-known fact is that at low frequencies, the Van Vleck — Weisskopf form better corresponds to the observed spectra than the Lorentz form.

In the frequency range from 0 to 10 cm^{-1} the considered absorption can, for convenience of qualitative consideration, be represented in the form of the product of empirical exponential functions often used for parametrization of the continuum absorption in the millimeter and submillimeter wavelength ranges [11, 22, 29]:

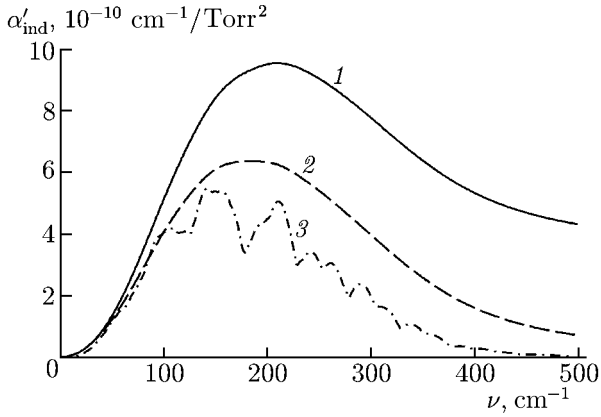

Fig. 3. The dependence of studied absorption (17) on the frequency ν for $T = 300$ K, which was obtained in this paper using the Van Vleck — Weisskopf line form (9) (solid curve *1*) and Lorentz line form (10) (dotted curve *2*). Curves *1* and *2* on the ordinate axis are scaled down by a factor of 10. The dependences obtained using truncated line forms (12) and (14) merge, with accuracy up to the line thickness, into one dash–dot curve *3*.

$$\gamma(\nu,P,T) = aP^2\,(T_0/T)^b\,\nu^c, \tag{18}$$

where $\gamma(\nu,T)$ is the absorption coefficient, a is a constant dimensional amplitude factor, and b and c are dimensionless exponents.

The simple form of temperature dependence (18) permits a qualitatively correct extrapolation of the result to the range of temperatures that are lower than the temperatures considered in [20]. This makes it possible to evaluate the studied component of the continuum under the Earth's atmosphere conditions.

TABLE 1. Parameters of Eq. (18) for the empirical modeling of absorption coefficient (17) in the frequency range 0–10 cm^{-1} for $T_0 = 300$ K using line forms (9), (10), and (12). Similar data on CIA from [12] and the total continuum absorption from [22] are given for comparison.

Parameters of Eq. (18)	Absorption coefficient (17) (300–700 K) obtained using			CIA [12] (240–330 K)	Total continuum absorption [22] (261–328 K)
	Van Vleck — Weisskopf form (9)	Lorentz form (10)	"truncated" Van Vleck — Weisskopf form (12)		
a, $10^{-14}\mathrm{cm}^{-1+c}\,\mathrm{Torr}^{-2}$	45.14	49.26	0.54	1.38	$2.93 \cdot 10^4$
b	3.94	3.95	5.98	4.45	8.24
c	2.01	2.00	2.29	2.29	2.00

The coefficients of function (18) are presented in Table 1 together with similar coefficients of the empirical parametrization of the continuum studied in other papers.

5. COMPARATIVE ANALYSIS OF THE DATA

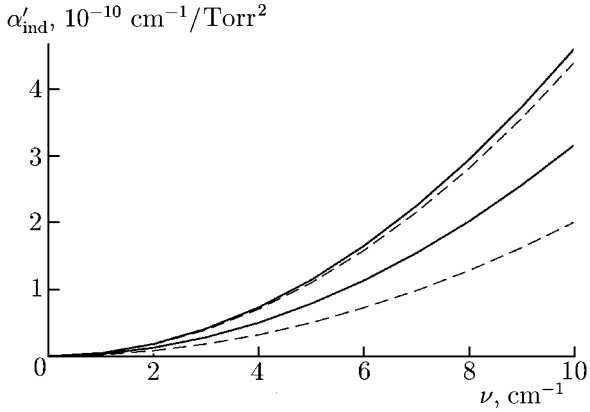

Fig. 4. Frequency dependences of the absorption coefficient (17) obtained using Van Vleck — Weisskopf line form (9) (solid curves) and a factor of 600 scaled-down continuum absorption in water vapor according to experimental data from [22] (dashed curves). The lower curves correspond to a temperature of 330 K and the upper curves, to 300 K.

To demonstrate the contribution of the studied mechanism of absorption of the radiation by water vapor into the continuum absorption we present two pairs of diagrams for the frequency range of 0 to 10 cm^{-1} (Fig. 4), which characterize the absorption coefficient variation in the temperature range from 300 to 330 K.

The first pair of diagrams reflects the frequency dependence of the part of the continuum in humid nitrogen, which is quadratic with respect to the partial pressure of water vapor, according to the experimental data from [22]. The latter are in good agreement with similar prior measurements [30, 31] and are therefore used in this study. The second pair corresponds to studied absorption (17).

Although this temperature range is related only to the warm surface layer of the atmosphere, the conclusions obtained in its analysis can be extrapolated to the range of lower temperatures. It is well known that the continuum absorption decreases with increasing temperature at a constant pressure. The studied-absorption model constructed in this paper on the basis of *ab initio* calculations for temperatures 300–700 K [20] also gives a decaying temperature dependence. The ratio of the studied absorption to the total continuum absorption increases with the temperature (see Table 1). Therefore, assuming that the temperature dependences of the studied and total continuum absorptions are retained at lower temperatures, we find that the contribution of the studied absorption to the continuum for the atmospheric conditions will be even lower.

It follows from Fig. 4 that in a temperature range of 300 to 330 K the absorption stipulated by the additional dipole moment induced as a result of a collision of two free molecules is negligible compared with the total continuum absorption. Moreover, according to our model, the amplitude of the studied effect is so insignificant that it seems too difficult to single out it against the background of the total continuum absorption when trying an experimental study under conditions close to the Earth's atmosphere

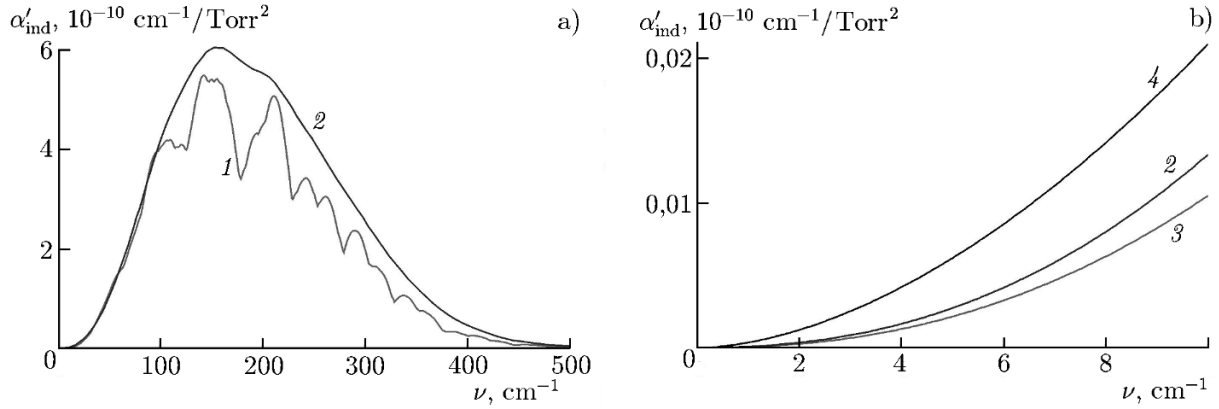

Fig. 5. (a) The frequency dependence of studied absorption (17), which was obtained in this paper using truncated line forms (12) and (14) (on this scale, they merge into one dotted curve *1*) and the spectrum taken from [12] solid curve *2*) for a frequency range of 0 to 500 cm^{-1} at $T = 300$ K. (b) Fragment of the spectra in a frequency range of 0 to 10 cm^{-1}. Line form (12) corresponds to the lower curve *3*, and line form (14), to the upper curve *4*.

environment. For example, for the partial pressure of saturated water vapor at a temperature of 273 K the absorption coefficient (17) corresponding to the effect studied in this paper will not exceed $1.5 \cdot 10^{-9}$ cm^{-1} in a frequency range of 0 to 10 cm^{-1}. The best sensitivity of the cavity spectrometers, which are currently used to study the absorption of this type is $8 \cdot 10^{-9}$ cm^{-1} [32].

The studied absorption as a component of the continuum has been considered by many authors [9, 12, 16, 31–36]. However, its qualitative estimation for water vapor under atmospheric conditions was performed, to our knowledge, only in two papers. The authors of [16] calculated the coefficient of absorption of electromagnetic radiation by the molecules of the main atmospheric gases, which is due to the dipole moments induced in binary collisions with water molecules. The authors of [12] analyzed the collision-induced absorption arising from the fact that "... during collisions of two interacting molecules, transient dipole moments occur and the latter can cause absorptions in the same way as permanent dipole moments do."

In [16], the collision-induced absorption was calculated at a temperature of 293 K and a water-vapor pressure of 15 Torr in the frequency range 0–60 cm^{-1}. The result of this calculation is in good agreement with the absorption estimated in this paper in the frequency range below 6 cm^{-1}. The absorption coefficient calculated using the full line form (9) differs from the results of [16] by less than twofold. In the high-frequency part of the considered frequency range, our model predicts a much higher absorption.

For comparison with the results of [12], in Fig. 5 we show the spectrum of the absorption (17), which we studied using truncated line forms (12) and (14) in a frequency range of 0 to 500 cm^{-1} at a temperature of 300 K, and the corresponding spectrum constructed on the basis of Fig. 6 from [12].

From the analysis of Figs. 3 and 5 it is seen that the studied absorption (17), which was found using the line forms (9), (10), (12), and (14), is in qualitative agreement with the absorption obtained in [12]. Figure 5b indicates that in the frequency range 0–10 cm^{-1}, despite the significant difference of the amplitudes, the frequency dependence of coefficient (17) qualitatively does not change when truncated line forms (12) or (14) are chosen.

For a numerical comparison of the results of this paper with the results of the study in [12], we used the frequency dependences presented in Fig. 6 of [12]. The coefficients of function (18), which correspond to these spectra in a frequency range of 0 to 10 cm^{-1} and a temperature range of 240 to 330 K, are given in Table 1. Among the truncated line forms in Table 1 only the data on the line form (12) are presented, since, according to [12], the use of the latter in this frequency range is more expedient.

The data of Table 1 is evidence that the choice of any of the classical line forms (9) or (10) for modeling of studied absorption (17) virtually does not affect the parametrization coefficients (18). Note

that the temperature dependence of the additional absorption studied in this paper using line forms (9) or (10) almost coincides with that studied in [12], where the authors of that paper also note that the main features of the CIA spectrum and its different temperature dependences near the band center and in the transparency window almost do not depend on the choice of the model of the resonant line form. The difference between the CIA from [12] and the studied absorption (17) depends on the choice of a classical or truncated line form in the absorption description. However, both the studied absorption (17) and the absorption calculated in [16], as well as CIA from the study in [12], are negligible compared with the total continuum absorption.

6. ALLOWANCE FOR THE COLLISIONAL DIMERIZATION OF MOLECULES

It was mentioned above that the absorption coefficient (17) corresponds to the contribution of free pairs of interacting molecules into the observed continuum absorption. When Eq. (17) was derived, it was assumed that the effect under study is contributed by each water-vapor molecule. This is equivalent to assuming that all the molecule pairs are free, i. e., neglecting the possibility of the formation of dimers from the molecules. The authors of [20], calculating the average dipole moment per water molecule, did not touch upon the problems of the formation of molecular complexes and their dissociation. However, it is well known that during the formation of a dimer the dipole moment of the monomers included in it increases [14, 37], and the number of pairs that form the dimers in collisions with respect to the number of free pairs can be significant, especially at low temperatures [9].

How much the studied absorption will change on account of the molecule dimerization possibility can be estimated from the number of resulting dimers and how much the average dipole moment of the H_2O molecule will change during the formation of the $(H_2O)_2$ dimer.

The average dipole moment per molecule, which was calculated in [20], is redistributed between the molecules that form free pairs and the molecules that form dimers as follows:

$$\mu(\rho,T) = \mu_0 + \Delta\mu = \frac{N_\mathrm{m}}{N}\mu_\mathrm{m} + \frac{2N_\mathrm{d}}{N}\mu_\mathrm{d} = \frac{N_\mathrm{m}}{N}(\mu_0 + \Delta\mu_\mathrm{m}) + \frac{2N_\mathrm{d}}{N}(\mu_0 + \Delta\mu_\mathrm{d}), \tag{19}$$

where μ_m and μ_d are the average dipole moments, and $\Delta\mu_\mathrm{m}$ and $\Delta\mu_\mathrm{d}$ are average dipole moments per H_2O molecule, which are additional to the moment μ_0, in monomers of free pairs and in dimers, respectively, N_m and N_d are the numbers of monomers and dimers in a gas, respectively, and $N = N_\mathrm{m} + 2N_\mathrm{d}$ is the total number of gas monomers, including those forming the dimers. The factor of two before the number N_d indicates that the dimer comprises a pair of monomers.

The average additional dipole moment per molecule in free pairs (assuming that $N_\mathrm{m} \approx N$) can be obtained from Eq. (19):

$$\Delta\mu_\mathrm{m} = \Delta\mu(\rho,T) - \frac{2N_\mathrm{d}}{N}\,\Delta\mu_\mathrm{d}. \tag{20}$$

Assuming that dimers and monomers are ideal gases and expressing the ratio P_d/P, where P_d is the partial pressure of dimers, through the partial pressure of water vapor and the dimer equilibrium constant, Eq. (20) can be rewritten as

$$\Delta\mu_\mathrm{m} = \Delta\mu(\rho,T) - 2K_\mathrm{d}(T)P\,\Delta\mu_\mathrm{d}. \tag{21}$$

We evaluate the additional dipole moment $\Delta\mu_\mathrm{d}$, which corresponds to one molecule of a monomer in the dimer as a function of temperature, on the basis of simple qualitative considerations. In the equilibrium dimer configuration corresponding to the temperature 0 K, the dipole moment per monomer molecule is 1.923 D [14] according to the *ab initio* data. Another characteristic temperature T_d at which the energy stored in the hydrogen bond stretching oscillations (kT) is equal to the dimer dissociation energy, which is 1105(10) cm^{-1} (1590 K) according to the experimental data [38], corresponds to the decay of a dimer into a pair of monomers. In this case, the dipole moment of a monomer as part of a dimer becomes close to μ_0, and the additional dipole moment, close to zero.

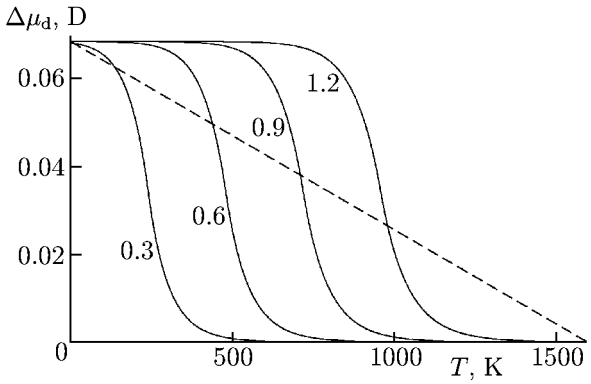

Fig. 6. Assumed form of dependence (23) of the additional dipole moment for one molecule of a monomer in the dimer (solid curves). Digits on the curves show the corresponding values of the parameter x. A simple linear dependence given by Eq. (22) is shown by dotted line.

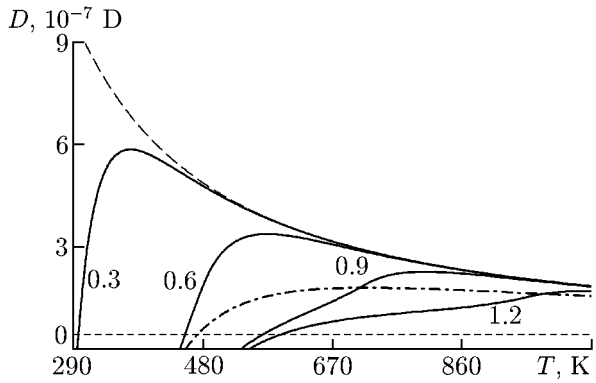

Fig. 7. Temperature dependence of the pressure-normalized additional dipole moment of water molecules (expression (25)) (solid lines correspond to a set of parameter values given in the figure: $x = 0.3$, 0.6, 0.9, and 1.2). The same dependence with linear approximation (22) (dash–dot line) and without the additional dimer formation (dashed curve). The zero value of D is shown by a dotted line.

These considerations do not allow for the metastable dimers whose internal energy is higher than the hydrogen bond dissociation energy. Since the lifetime and the additional dipole moment per molecule of a metastable dimer is less than that of a stable dimer, most of the metastable dimers can be qualified as free pairs for such estimates.

Assuming that the average dipole moment per H_2O molecule in the dimer changes in direct proportion to the temperature, we find that

$$\Delta\mu_{\rm d}^{\rm line}(T) = (\mu_{\rm d} - \mu_0)\,(1 - T/T_{\rm d}). \tag{22}$$

The actual dependence $\Delta\mu_{\rm d}(T)$ is not known. Of course, this dependence is nonlinear and is not described by Eq. (22). More probably, it resembles a linear combination of exponents increasing and decreasing in T (sometimes this combination is called a switching function), which satisfies the above-described boundary conditions for $T = 0$ and $T = T_{\rm d}$. The qualitative form of the function $\Delta\mu_{\rm d}(T)$ can be established from common properties of the interaction potential of a pair of water monomers that form the dimer. Near the potential well, i. e., at low temperatures, the oscillations of monomers are almost harmonic and the dipole moment is constant on the average, i. e., the desired dependence has a nearly zero derivative. As the temperature increases, the oscillation amplitude rises rapidly, which causes an anharmonism increase. The temperature derivative of the dipole moment, which is negative, increases in absolute value. When the oscillations become so large that the flat attractive wing of the interaction potential comes into effect, the magnitude of the dipole-moment variation rate of a monomer in the dimer drops, so that before the dissociation the desired temperature dependence has again a nearly zero derivative.

As the dependence approximately satisfying the described properties, we use the function

$$\Delta\mu_{\rm d}^{\rm sw}(x,T) = \begin{cases} \dfrac{(\mu_{\rm d} - \mu_0)\,\{2 - \exp[b(T)\,(T - xT_{\rm d}/2)]\}}{2}, & T < xT_{\rm d}/2; \\ \dfrac{\mu_{\rm d} - \mu_0}{2}\exp[-b(T)\,(T - xT_{\rm d}/2)], & T > xT_{\rm d}/2, \end{cases} \tag{23}$$

where

$$b(T) = 0.02 - 0.01\sqrt{T/T_{\rm d}}. \tag{24}$$

The dependence of the average dipole moment per monomer in the dimer, in accordance with function (23) for the parameter x ranging from 0.3 to 1.2 gives the curves shown in Fig. 6.

Consider the right-hand side of Eq. (21) normalized to the pressure P:

$$D(T) = \frac{\Delta\mu(\rho,T) - 2K_{\rm d}(T)P\,\Delta\mu_{\rm d}(T)}{P(T)}, \tag{25}$$

which represents a pressure-normalized average additional dipole moment per monomer molecule not included into the dimer. To evaluate the dependence of the dimerization constant on the temperature T, we use an empirical expression obtained on the basis of *ab initio* calculations in [39]. However, it should be taken into account that the dimer association energy equal to 1234 cm^{-1} (1777 K), which was used in the dependence, is overestimated compared to the values measured experimentally in [38], which amount to 1105(10) cm^{-1} (1590 K). Since the dependence $K_{\rm d}(T)$ is proportional to $\exp[D_0/(kT)]$, where D_0 is the dimer dissociation energy, the dimerization constant from [39] should be multiplied by a temperature-independent coefficient, $\exp[-\Delta D_0/(kT)]$, where $\Delta D_0 = 1234$ cm^{-1} $-$ 1105 cm^{-1} = 129 cm^{-1}.

The temperature dependence of function (25) for different values of the parameter x is presented in Fig. 7. In this figure, it is shown for comparison how this function looks like for $K_{\rm d} = 0$ (dotted curve), i. e., assuming that the dimers are not formed.

Figure 7 shows that, despite the very small relative fraction of dimers in water vapor (in saturated water vapor at 300 K, there is only one dimer per about one thousand monomer molecules), they correspond to quite a significant fraction of the additional dipole moment. In this case, the form of the temperature dependence of the average dipole moment of a monomer in the dimer is of fundamental importance. Anyway, as follows from Fig. 7, allowance for the molecule dimerization leads to a limiting temperature, below which it does not make sense to speak of the studied absorption (dependence (25) is zero). This temperature corresponds to the case where the entire average additional dipole moment per one H_2*case*O molecule in water vapor, which results from intermolecular interactions, should be attributed to bound dimers. The boundary temperature is very strongly dependent on the rate at which the hydrogen bond in the dimer becomes weak as the temperature rises. When the parameter x in Eq. (23) ranges from 0.3 to 1.2 (which corresponds to the extreme curves in Fig. 6), the limiting temperature varies from 297 to 594 K.

Thus, allowance for the water molecule dimerization eliminates the contribution of the additional collisional polarization of the water molecules into the continuum absorption of millimeter and submillimeter waves by water vapor under atmospheric conditions.

This conclusion also conforms to the results of [9], where it is stated that in the Earth's atmosphere, free states of the molecule pairs are virtually absent. It should be mentioned that, according to [9], free pairs of water molecules start to be manifested at a temperature equal to about 540 K, which approximately agrees with the limiting temperature resulting at average values of the parameter x in Eq. (23) (Fig. 7). Since, as was mentioned, the source of the studied absorption is strong inelastic interactions of molecules in the state of free pairs, the absence of free pairs under atmospheric conditions means the absence of this mechanism of the radiation absorption.

7. DISCUSSION

The modeling conditions in [20] are quite exotic, and the use of the data obtained in that paper for the construction of the dipole-moment dependence $\mu(\rho,T)$ requires additional substantiation. The authors of [20] model the liquid phase, rather than the gas. However, the difference between these two phases, especially at supercritical temperatures, which were also considered in that study, is only conventional and mainly consists in different distances between the molecules. Liquids have the so-called short-range order of the molecules and a quasi-crystalline lattice with the monomers oscillating at the nodes. However, this

lattice, which is formed due to hydrogen bonds between individual monomers [40], is quite dynamic. Because of the thermal motion, the established hydrogen bonds are continuously broken in each molecule and new hydrogen bonds with the neighboring molecules are formed. Moreover, it is well known that in liquid water, even covalent bonds between the oxygen and hydrogen atoms are broken because of the intermolecular forces, resulting in a continuous proton exchange between molecules, which occurs at room temperature over a time of the order of only about $6 \cdot 10^{-4}$ s [41], although the energy of these bonds is more than 41000 cm^{-1}. The energy of hydrogen bond in, e. g., a water dimer, is only about 1100 cm^{-1} [38, 42]. This means that the time of existence of a quasi-crystalline lattice in liquid water is very short. Therefore, on short time intervals, liquid water can be regarded as a very strongly compressed gas.

The authors of [18] note that in the modeling, the diffusion of molecules is almost absent and fast re-orientations are the main form of their motion. With allowance for this comment, it can be assumed that a collision of two monomers is due to oscillations of the molecules at the nodes of a quasi-crystalline lattice, which, in view of rapid re-orientations being an analog of rotation, is equivalent to random collisions of molecules in a gas. Based on this analysis, as well as on the arguments given in Sec. 2, we think it is justified to extrapolate the data given in [20] to the range of lower densities.

Another approximation we used in this paper is that as the basis of calculation, we use the rotational spectrum of absorption of a water molecule in the dipole approximation, which implies that the selection rules have the form $\Delta J = 0, \pm 1$, where J is the rotational quantum number. This spectrum is well studied and easy to model. However, this means that a number of assumptions are adopted. First of all, the molecule deformation related to a tangible effect of the collision partner fields is neglected. This is justified by the fact that under normal conditions, the average translational kinetic energy $3kT/2$ of the molecules is of the order of 300 cm^{-1}, which is significantly less than even the energy of excitation of kink oscillations in the water molecule (about 1800 cm^{-1}). It is also well known that in the absorption spectra of non-polar molecules, which are due to their collisional interaction, there are transitions with varied rotational number $\Delta J = \pm 2$ [23, 42, 43].

That only conventional electric-dipole rotational lines can be used for the absorption spectrum modeling is supported by an analogy between the molecular transitions due to radiation and the transitions due to collisions. In accordance with the classical approach to the collisional interaction of molecules (see [45]), the result of interaction is similar to the pulse action of the field. The probability of transition of a molecule to another level will be nonzero if the pulse spectrum has a nonzero amplitude at the frequency of the corresponding line.

The question on which levels the molecule transits to in collisions, i. e., under the action of such a pulse, has been considered in a series of papers [46–48]. In those studies, it was found experimentally that in polar molecules, the transitions stimulated by inelastic intermolecular collisions that change the rotational state of a molecule, mainly obey the selection rules for electric-dipole transitions, i. e., the transitions with varied rotational number $\Delta J = 0, \pm 1$ dominate. The probability of all other transitions, including those in which $\Delta J = \pm 2$ is also nonzero. The latter depends on the particular pair of colliding molecules, but the transitions with $\Delta J = 0, \pm 1$ dominate.

It should be mentioned that, as in the present paper, the authors of [12], whose results we use for comparison with our study, rely on ordinary electric-dipole transitions, with the parameters taken from the data base [21], when considering CIA in the range of a purely rotational spectrum of H_2O.

Another argument in favor of using the rotational spectrum of molecule absorption in the dipole approximation for the model construction is the statement in [44] saying that "A substance in a strong electric field acquires a new infrared spectrum owing to changes in the selection rules... Of course the ordinary infrared spectrum due to M_{sigma} [matrix components of a (constant) dipole moment] will be present perhaps with very small shifts due to a small Stark effect shift of the levels."

We also note that the selection rules do not affect the overall picture of the rotational spectrum of the molecule absorption, which is observed, for example, at large pressures, when individual rotational lines merge into bands. The form of such bands is determined only by the rotational constants of a molecule,

and the distribution of molecules over rotational energy levels, which is controlled by the gas temperature.

All this means that upon collisions, the general form of the rotational spectrum of molecule absorption will be about the same as for isolated molecules during a very short time of interaction with the field.

8. CONCLUSIONS

In the course of this work, we have analyzed the absorption of electromagnetic radiation in water vapor, which arises due to the additional polarization of molecules (the dipole moment induced in them) as a result of binary collisions. Based on the *ab initio* data [20] about the average dipole moment of a water molecule as a function of density and temperature, we developed a model for calculation of the additional absorption coefficient corresponding to the effect analyzed. In the approximation of an ideal gas (i. e., non-coalescing molecules) for the model of absorption in the millimeter and submillimeter wavelength ranges, we obtained an empirical analytical expression for the absorption coefficient in a temperature range of 300 to 700 K, which permits one to extrapolate the obtained result to the range of lower temperatures that are typical of the Earth's atmosphere. Comparison of the model absorption with the experimental data suggests that the contribution of the additional absorption mechanism examined in this paper is negligible under the atmospheric conditions. Absorption in the approximation of absence of dimers in water vapor is in qualitative and quantitative agreement with the results obtained in [12] and [16]. Allowance for the dimerization of the colliding gas molecule moved the "region of existence" of the studied mechanism towards the range of higher temperatures, making its contribution to the atmospheric continuum absorption even less significant, in agreement with the conclusions of [9].

A practical conclusion of this paper is that the studied effect can be ruled out in the analysis of experimental spectra of the continuum absorption in water vapor under conditions typical of the Earth's atmosphere [17, 49].

The authors express their gratitude to A. A. Vigasin for multiple long discussions on the subject and his valuable advices. This work was supported in part by the Russian Foundation for Basic Research. The work of M. Yu. Tretyakov was supported by a grant under Agreement No. 02.V.49.21.0003 of August 27, 2013 between the Ministry of Education and Science of the Russian Federation and the N. I. Lobachevsky State University of Nizhny Novgorod.

REFERENCES

1. J. T. Kiehl and K. E. Trenberth, *Bull. Amer. Meteorol. Assoc.*, **78**, 197 (1997).
2. I. M. Held and B. J. Soden, *Ann. Rev. Energy Environ.*, **25**, 441 (2000).
3. R. V. Leslie and D. H. Staelin, *IEEE Trans. Geosci. Remote Sensing*, **42**, No. 10, 2240 (2004).
4. J. R. Wang, L. A. Chang, B. Monosmith, et al., *IEEE Trans. Geosci. Remote Sensing* **46**, No. 1, 137 (2008).
5. S. M. I. Azeem, S. E. Palo, D. L. Wu, et al., *Geophys. Res. Lett.*, **28**, 3147 (2001).
6. F. T. Barath, M. C. Chavez, R. E. Cofield, et al., *J. Geophys. Res. Atmos.*, **98**, No. D6, 10751 (1993).
7. D. L.Wua, M. J. Schwartza, J. W. Watersa, et al., *Adv. Space Res.*, **42**, No. 7, 1246 (2008).
8. D. E. Stogryn and J. O. Hirschfelder, *J. Chem. Phys.*, **31**, No. 6, 1531 (1959).
9. A. A. Vigasin, *Infrared Phys.*, **32**, 461 (1991).
10. A. A. Vigasin, in: C. Camy-Peyret and A. A. Vigasin, eds., *Weakly Interacting Molecular Pairs: Unconventional Absorbers of Radiation in the Atmosphere*, Kluwer Acad. Publ., Netherlands (2003), p. 23.
11. H. P. Liebe, *Int. J. Infrared Millimeter Waves*, **5**, No. 2, 207 (1984).
12. C. Leforestier, R. H. Tipping, and Q. Ma, *J. Chem. Phys.*, **132**, 164302 (2010).

13. Q. Ma, T. H. Tipping, and C. Leforestier, *J. Chem. Phys.*, **128**, 124313 (2008).
14. Y. Scribano and C. Leforestier, *J. Chem. Phys.*, **126**, 234301 (2007).
15. A. A. Viktorova and S. A. Zhevakin, *Dokl. Akad. Nauk SSSR*, **171**, No. 5, 1061 (1966).
16. K. P. Gaikovich and A. P. Naumov, *Radiotekh. Élektron.*, **25**, No. 8, 1763 (1980).
17. M. Yu. Tretyakov, M. A. Koshelev, E. A. Serov, et al., *Phys. Usp.*, **57**, No. 11, 1083 (2014).
18. K. P. Shine, I. V. Ptashnik, and G. Radel, *Surv. Geophys.*, **33**, Nos. 3–4, 535 (2012).
19. S. A. Clough, Y. Beers, G. P. Klein, et al., *J. Chem. Phys.*, **59**, 2254 (1973).
20. T. Ikeda, Y. Katayama, H. Saitoh, et al., *J. Chem. Phys.*, **132**, 121102 (2010).
21. L. S. Rothman, I. E. Gordon, Y. Babikov, et al., *J. Quant. Spectrosc. Radiat. Transfer*, **130**, 4 (2013).
22. M. A. Koshelev, E. A. Serov, V. V. Parshin, et al., *J. Quant. Spectrosc. Radiat. Transfer*, **112**, 2704 (2011).
23. J. M. Hartmann, C. Boulet, and D. Robert, *Collisional Effects on Molecular Spectra*, Elsevier, Amsterdam (2008).
24. I. V. Ptashnik, K. P. Shine, and A. A. Vigasin, *J. Quant. Spectrosc. Radiat. Transfer*, **112**, 1286 (2011).
25. F. A. Hamprecht, A. J. Cohen, D. J. Tozer, et al., *J. Chem. Phys.*, **109**, 6264 (1998).
26. M. Yu. Tretyakov, E. A. Serov, and T. A. Odintsova, *Radiophys. Quantum Electron.*, **54**, No. 10, 700 (2011).
27. C. Leforestier, *J. Chem. Phys.*, **140**, 074106 (2014).
28. J. H. Van Vleck and V. F. Weisskopf, *Rev. Mod. Phys.*, **17**, Nos. 2–3, 227 (1945).
29. A. Bauer, N. Godon, J. Carlier, et al., *J. Quant. Spectrosc. Radiat. Transfer*, **59**, Nos. 3–5, 273 (1998).
30. H. J. Liebe and D. H. Layton, *Millimeter-Wave Properties of the Atmosphere: Laboratory Studies and Propagation Modeling: NTIA Report*, Nos. 87-224 (1987).
31. T. Kuhn, A. Bauer, M. Godon, et al., *J. Quant. Spectrosc. Radiat. Transfer*, **74**, 545 (1974).
32. M. Yu. Tretyakov, A. F. Krupnov, M. A. Koshelev, et al., *Rev. Sci. Instrum.*, **80**, 093106 (2009).
33. E. J. Mlawer, S. A. Clough, P. D. Brown, et al., in: *Proc. 8th Atmospheric Radiation Measurement (ARM) Science Team Meeting, US Department of Energy, Washington* (1998).
34. A. Bauer and M. Godon, *J. Quant. Spectrosc. Radiat. Transfer*, **69**, 277 (2001).
35. S. A. Clough, M. W. Shephard, E. J. Mlawer, et al., *J. Quant. Spectrosc. Radiat. Transfer*, **91**, 233 (2005).
36. Yu. I. Baranov and W. J. Lafferty, *Phil. Trans. Roy. Soc.*, **370**, 2578 (2012).
37. J. K. Gregory, D. C. Clary, K. Liu, et al., *Science*, **275**, 814 (1997).
38. B. E. Rocher-Casterline, L. C. Ch'ng, A. K. Mollner, et al., *J. Chem. Phys.*, **134**, 211101 (2011).
39. Y. Scribano, M. Goldman, R. J. Saykally, et al., *J. Phys. Chem. A*, **110**, 5411 (2006).
40. A. J. Huneycutt and R. J. Saykally, *Science*, **299**, 1329 (2003).
41. R. R. Knispel and M. M. Pintar, *Chem. Phys. Lett.*, **32**, No. 2, 238 (1975).
42. C. Leforestier, K. Szalewicz, and A. van der Avoird, *J. Chem. Phys.*, **137**, 014305 (2012).
43. H. Hermann, W. H. Christoph, and W. D. Brewer, *Molecular Physics and Elements of Quantum Chemistry*, Springer (2004).
44. E. U. Condon, *Phys. Rev.*, **41**, 759 (1932).

45. C. H. Townes and A. L. Schawlow, *Microwave Spectroscopy*, McGraw-Hill, New York (1966).
46. T. Oka, *J. Chem. Phys.*, **1966**, 45, 754 (1966).
47. T. Oka, *J. Chem. Phys.*, **47**, No. 1, 13 (1967).
48. T. Oka, *J. Chem. Phys.*, **48**, No. 11, 4919 (1968).
49. M. Yu. Tretyakov, E. A. Serov, M. A. Koshelev, et al., *Phys. Rev. Lett.*, **110**, 093001 (2013).